

## Morphological and chemical instabilities of nitrogen delta-doped GaAs/(Al,Ga)As quantum wells

E. Luna<sup>1\*</sup>, R. Gargallo-Caballero<sup>1</sup>, F. Ishikawa<sup>2,3</sup>, and A. Trampert<sup>1</sup>

<sup>1</sup>Paul-Drude-Institut für Festkörperelektronik, Hausvogteiplatz 5-7, 10117 Berlin, Germany

<sup>2</sup>Graduate School of Engineering, Osaka University, 2-1 Yamadaoka, Suita, Osaka 565-0871,

Japan

<sup>3</sup>Graduate School of Science and Engineering, Ehime University, 3 Bunkyo-cho, Matsuyama,

Ehime 790-8577, Japan

The microstructure and the element distribution across tensile-strained nitrogen  $\delta$ -doped GaAs/(Al,Ga)As quantum wells (QW) is investigated by transmission electron microscopy. We find that the nitrogen sub-monolayer insertion results in a several monolayer thick Ga(As,N) layer with thickness and lateral composition fluctuations. The thickness and composition fluctuations are not arbitrary but they are anticorrelated, i.e. the Ga(As,N) layer is thinner in areas of higher nitrogen content and vice versa. Thus, regardless of the specific position *along* the QW, the amount of incorporated nitrogen remains constant and close to its nominal value. The increase of the nitrogen content at the insertion promotes an anisotropic shape transition towards highly-faceted three-dimensional structures. Our experimental observations indicate that the two-dimensional to three-dimensional morphological transition is determined by intrinsic factors associated with the different Ga-N and Ga-As bonds and hence occurs regardless of the epitaxial strain state of the layers.

**Keywords** — dilute nitrides, delta-doping, transmission electron microscopy

---

\* Corresponding author: [luna@pdi-berlin.de](mailto:luna@pdi-berlin.de)

The incorporation of a few percent nitrogen in III–V compound semiconductors, the so-called dilute nitrides, has attracted much attention due to the peculiar and significant changes in the local electronic structure of the host semiconductor. In particular, the incorporation of small amounts of nitrogen is very effective in reducing the band gap, acting primarily on the conduction band and leaving the valence band almost unaffected, which in turn opens the possibility to get access to longer wavelengths and extend the capabilities for technologically important optoelectronics.<sup>1–3</sup> Dilute nitrides are highly-mismatched alloys (HMA), which are formed by the substitution of isoelectronic elements with very different size and/or electronegativity. As a consequence, HMA are often affected by a miscibility gap, which makes their growth challenging due to the tendency of the alloy to phase separate. Morphological instabilities due to decomposition-driven nanometer-sized compositions fluctuations have been reported in (In,Ga)(As,N) and Ga(As,N).<sup>4–10</sup> It was demonstrated that the origin of such morphological instabilities is not the accumulation of *macroscopic epitaxial strain*.<sup>6–10</sup> Instead, the observed surface roughening, which in extreme cases leads to a two-dimensional (2D) to three-dimensional (3D) transition, seems to arise from *local strains* due to the preferred formation of Ga-N and In-As bond configurations.<sup>7,8</sup>

In order to incorporate nitrogen in an atomically-controlled way, in recent years some groups have developed growth methods based on site-controlled nitrogen  $\delta$ -doping techniques using molecular beam epitaxy (MBE).<sup>11–16</sup> While in conventional MBE growth of dilute nitrides the species are continuously supplied, the idea behind  $\delta$ -doping is to create an atomically-controlled nitrogen sheet embedded in a III–As matrix via surface nitridation, e.g. by nitrogen irradiation in plasma-assisted MBE.<sup>12–14</sup> Although this innovative approach was originally proposed to explore the concept of single-photon emission from individual N-related impurity centers,<sup>11,12</sup> it is clear that the properties of quantum structures such as quantum wells (QWs) and superlattices (SLs) can be significantly affected by nitrogen sub-monolayer

insertions. As a matter of fact, the demonstrated feasibility of band gap engineering by nitrogen  $\delta$ -doping<sup>17,18</sup> has opened up new alternatives, such as its use in intermediate-band solar cells,<sup>18,19</sup> aside from those works reporting a significant improvement in the optical properties and material quality of Ga(As,N) pseudo-alloys.<sup>13,15,16</sup>

The electronic states created by the N-related centers cause substantial localization of excitons. In the impurity limit, the localized electronic states related to N-pairs give rise to a series of distinct, strong and extremely narrow luminescence lines.<sup>11,12,20,21</sup> Furthermore, these electronics states, and hence the emission wavelengths, are uniquely determined by the combination of host material and impurity center, making them good candidates as single photon emitters as shown in recent works where single-photon emission from GaAs:N<sup>22</sup> and AlAs:N<sup>21</sup> has been demonstrated. Nevertheless and despite extensive work, the exact origin of the narrow luminescence emission still remains under investigation.<sup>22-25</sup> Regarding the prospects of band gap engineering, reports on nitrogen  $\delta$ -doped (In,Ga)As QWs have revealed a precise control of the emission wavelength by adjusting the nitrogen irradiation time.<sup>13-15</sup> More recently, investigations on ideal intermediate band materials demonstrate that SL structures consisting of alternating layers of undoped and nitrogen  $\delta$ -doped GaAs are more promising candidates for the absorber of intermediate band solar cells than Ga(As,N) alloys with uniform nitrogen incorporation,<sup>18,19</sup> since the GaAs:N  $\delta$ -doped SLs show enhanced optical transitions compared to uniformly incorporated Ga(As,N) alloys.<sup>18</sup> Whereas most of these investigations aim to gain a further insight into the band structure of the material, only few works have been devoted to study the microstructure of the nitrogen sub-monolayer insertion. When nitrogen is introduced using the site-controlled  $\delta$ -doping techniques, critical questions arise such as the truly nitrogen distribution. Furthermore, the formation mechanism of nitrogen  $\delta$ -doped layers is not yet fully understood.<sup>26</sup> In particular, it is crucial to determine whether the nitrogen is spatially constrained in a sub-monolayer structure (an unlikely

situation<sup>27</sup>) or whether it spreads out along the growth direction, as is indirectly suggested by recent experimental data<sup>17,19,25,28</sup> and is directly shown in the scarce works aimed to determine the truly nitrogen distribution.<sup>29,30</sup> In addition, a detailed knowledge of the impact of the nitrogen insertion on the structural properties of the surrounding matrix is required.

In this letter, we investigate the microstructure and element distribution of nitrogen  $\delta$ -doped GaAs/(Al,Ga)As QWs using transmission electron microscopy (TEM) techniques. In particular, the analysis is based on  $g_{002}$  dark-field TEM (DFTEM), which is a powerful technique to detect small variations in the composition at the nm scale.<sup>10,31–33</sup> Moreover,  $g_{002}$  DFTEM allows access to relatively large areas (hundreds of nm) within one single TEM specimen, thus allowing statistical TEM investigations and a reliable overview of the main features.<sup>10,33,34</sup> The information obtained using  $g_{002}$  DFTEM is thus complementary to the one provided by other techniques probing highly-spatially localized areas, such as cross-sectional scanning tunneling microscopy (STM).<sup>30</sup> Our analysis reveals that the intended nitrogen  $\delta$ -doped layer is in reality a several monolayer (ML) thick Ga(As,N) layer with lateral composition fluctuations and inhomogeneous thickness. Additionally, we observe that the increase in the nitrogen content at the insertion promotes an anisotropic shape transition towards highly-faceted 3D structures.

The samples were grown on semi-insulating GaAs (001) substrates using plasma-assisted MBE. Conventional effusion cells were used for Ga and Al and a two-zone cracker source was used for As<sub>2</sub>. Nitrogen  $\delta$ -doping was carried out by nitrogen plasma irradiation during a growth interruption in the center of an 8 nm GaAs QW sandwiched by 180 nm (Al,Ga)As barriers. The substrate temperature  $T_s$  was 560°C and the As beam equivalent pressure was  $8 \times 10^{-6}$  Torr. Both,  $T_s$  and the As pressure are predicted to strongly affect N incorporation.<sup>35</sup> The amount of introduced nitrogen was controlled by the irradiation time, yielding a nitrogen coverage on the growth front of up to 0.5 ML. In particular, the nitrogen

coverage of the investigated samples varied between 0.12 and 0.5 ML. Further growth details can be found elsewhere.<sup>17</sup>

Cross-sectional TEM foils were prepared in the [110] and  $[1\bar{1}0]$  projections using mechanical thinning followed by Ar-ion milling. In order to minimize the sputtering damage, the Ar-ion beam energy was reduced to about 1.5 keV for the final milling step. TEM investigations were carried out using a Jeol JEM 3010 microscope operating at 300 kV equipped with a GATAN slow-scan CCD camera. Our analyses of the composition are based on  $g=002$  DFTEM imaging, which is highly sensitive to variations in the chemistry of the alloy in semiconductors with zincblende (ZB) structure. The reason is that in III–V alloys with ZB structure, the diffracted intensity for the 002 reflection under kinematic approximation is proportional to the square of the structure factor, which in turn depends on the difference in the atomic-scattering factors of the alloy components.<sup>34,36</sup> Therefore, in this “structure-factor imaging mode”, the contrast mainly arises from differences in the atomic-scattering factors between the group-III and group-V elements. Besides, strain may also affect the diffraction contrast. The effect of strain mainly reflects on thin-foil relaxation, on dynamical contributions from non systematic row reflections and on the impact of static atomic displacements.<sup>36-38</sup> When 002 imaging conditions are properly set up to minimize dynamical contributions from strain-sensitive reflections (the specimen was tilted  $8-10^\circ$  from the  $\langle 110 \rangle$  zone axis towards the [100] pole, while keeping the interface edge-on<sup>34</sup>) for a specimen region of interest with thickness between 50–80 nm (to minimize the effects of thin foil relaxation) the contrast directly reflects the chemical composition of the alloy and can be used to estimate the element distribution assuming substitutional incorporation of N at As positions and the validity of Vegard’s law.<sup>33,34,36</sup> The influence of electron redistribution due to the bonding of atoms and of local structural distortions due to static atomic displacements are not considered here since

these refinements are within the experimental error for the low nitrogen contents ( $< 2.5\%$ ) considered in our quantitative analysis.<sup>38</sup>

Figure 1(a) shows a  $g_{002}$  DFTEM image of a GaAs QW with a sub-monolayer nitrogen insertion in the center of the QW. In this sample, the nominal amount of nitrogen at the insertion is 0.12 ML. Figure 1(b) displays a micrograph of a GaAs/(Al,Ga)As reference sample without the insertion. As observed in Figure 1(a), the presence of the insertion is clearly identified as a dark line at the center of the QW, indicating that the nitrogen  $\delta$ -doped layer is actually spread out over several ML (about 7 ML) along the growth direction, resulting in a well-defined Ga(As,N) layer of about 2 nm width. This width is on the same order as the narrow profiles obtained by truly  $\delta$ -doping in semiconductor structures.<sup>27</sup> It is also consistent with previous works which assumed that the nitrogen  $\delta$ -doped and the neighboring GaAs behave as a thin (Ga,As)N layer with a certain effective width<sup>18</sup> or with those works which, based on optical measurements, address the plausible existence of N-pairs configurations extending along the growth direction.<sup>23</sup> The composition determined using  $g_{002}$  DFTEM yields an averaged nitrogen content in the Ga(As,N) layer of about 1.7%. Estimate of the amount of incorporated nitrogen, computed as the product of the nitrogen concentration [N] by the nitrogen profile width  $W_N$ , i.e. in % ML units,<sup>27</sup> yields  $[N] \cdot W_N \sim (11.6 \pm 0.9) \% \text{ ML}$ , in good agreement with the nominal value of 12% ML. While the reference sample consists of a GaAs/(Al,Ga)As QW homogeneous in thickness and composition and with smooth interfaces [cf. Figure 1(b)], we find that the introduction of the nitrogen insertion results in a slight roughening of the GaAs-on-Ga(As,N) interface and in moderate QW thickness and lateral composition fluctuations. The fluctuations in the QW thickness,  $W$ , correlates with fluctuations in the  $\delta$ -doping width,  $W_N$ , as shown in Figures 2(a) and (b), which represent  $W$  and  $W_N$  values taken at different positions *along* the QW at a distance of about 20–50 nm each. The lateral composition fluctuations refer to the spatial variation of the nitrogen content along the

insertion. This is not the first time that the question of the *in-plane* compositional homogeneity comes into consideration for this kind of structures. Based on optical measurements, some authors suggested the existence of an inhomogeneous nitrogen distribution in the (001) growth plane.<sup>39</sup> We find that the lateral spatial variation of the nitrogen distribution is not arbitrary but there is an anticorrelation between  $[N]$  and  $W_N$  as observed in Figures 2(b) and (c):  $W_N$  is smaller in areas of higher  $[N]$  and vice versa, areas with low  $[N]$  extend over a larger  $W_N$ . Note that, regardless of the specific position *along* the QW, the product  $[N] \cdot W_N$  always remains close to the nominal value of 12% ML. Detailed information on the nitrogen profile can also be inferred from  $g_{002}$  DFTEM micrographs. Figure 3(b) displays an intensity line-scan obtained from the area marked in Figure 3(a), the image corresponds to the 0.12 ML-insertion sample. Macroscopic, epitaxial strain effects on the  $g_{002}$  DFTEM contrast would manifest as a diffuse band in the vicinity of the Ga(As,N) layer, in the barrier area.<sup>37,38</sup> In this case, however, we did not detect such diffuse band in any of the investigated samples. Thus, following the approach by Bithell and Stobbs<sup>36</sup> and using GaAs as reference, we determine the actual nitrogen distribution profile arising from the insertion, as displayed in Figure 3(c). The spread of the  $\delta$ -doping along the growth direction is very obvious, as well as the unavoidable interface broadening.<sup>40</sup> In addition, we detect an unintentional background in the nitrogen profile (at the lower part of the QW, before the insertion) up to  $[N] \sim 0.3\%$ , which was previously determined using secondary ion mass spectrometry<sup>17</sup> and arises from the unintentional incorporation of residual nitrogen in the MBE chamber after ignition of the plasma source.<sup>41,42</sup>

Increasing the amount of nitrogen at the insertion enhances the roughening and the QW thickness and composition fluctuations, as observed in Figure 4, which displays  $g_{002}$  DFTEM micrographs of a GaAs QW with a 0.5 ML insertion. Again, the presence of the nitrogen  $\delta$ -doping is clearly identified as a dark line since it spreads out along the growth direction creating a 10 ML thick Ga(As,N) layer with about 5% nitrogen. Notice the strong roughening

at the (Al,Ga)As-on-GaAs interface, i.e. after the insertion. Interestingly, we find that this roughening is anisotropic, hence the layers morphology is different when observed along the two perpendicular  $\langle 110 \rangle$  directions, as shown in Figure 4. As observed, while Figure 4(a) displays a rough 2D QW, TEM observations along the perpendicular projection [cf. Figure 4(b)] reveal the presence of highly-faceted 3D nanostructures. The shallow facets are close to the  $\{210\}$  and  $\{311\}$  planes. These results agree with previous observations on the formation of 3D structures following nitrogen irradiation<sup>16,18,26</sup> and are consistent with studies on the roughening of the GaAs overlayer using reflection high-energy electron diffraction.<sup>26</sup> A similar anisotropy has been reported for Ga(As,N) epilayers (no  $\delta$ -doping) grown by metalorganic (MO)MBE.<sup>5</sup> Moreover, a 2D-3D transition has been addressed in conventionally grown (i.e. with continuous N supply) (In,Ga)(As,N) and Ga(As,N) epilayers and QWs.<sup>5-10</sup> It occurs irrespective of the epitaxial strain state with the substrate (compressive or tensile), the growth technique (MBE, metal organic vapor phase epitaxy, MOMBE) and, in many cases, small changes in  $T_s$  or As-flux during growth are sufficient to trigger the transition process.<sup>10,31</sup> Hence the phenomenon is considered an intrinsic property of dilute nitride materials.<sup>6-10</sup> Furthermore, the occurrence of the 2D-3D transition is correlated with the presence of nanometer-sized composition modulations<sup>6-8</sup> and *local strains* due to the preferred formation of specific bond configurations.<sup>7,8</sup> The GaAs QW with the 0.5 ML insertion exhibits strong thickness and composition fluctuations with a periodicity of about 25–40 nm. The severe surface roughening renders a *quantitative* analysis of the N distribution in this sample unreliably [cf. Figs 2 and 3] since the imaging conditions may locally strongly deviate from  $\mathbf{g}_{002}$  DFTEM due to the local deformation of the atomic planes. Furthermore, the effect of static atomic displacements may not be negligible for higher [N].<sup>38</sup> Qualitative measurements are nevertheless possible and we find definite indications of lateral composition modulations as observed in the  $\mathbf{g}_{002}$  micrograph in Fig 4(c) displaying two intensity line-scans parallel to the

QW performed along the nitrogen insertion and the underneath GaAs, respectively. The modulation in the contrast along the insertion (i.e. in the N content) is obvious and indicates the alternating presence of N-rich and N-poor regions. Interestingly, using cross-sectional STM, Goldman *et al.* found laterally inhomogeneous GaN signatures after nitridation of a GaAs surface.<sup>4</sup> Such bond configurations are driven by maximizing the cohesive bond,<sup>7</sup> and GaN has higher cohesive energy (2.24 eV/bond) than GaAs (1.63 eV/bond).<sup>43</sup> Incidentally, we find a stronger roughening at the location of the N-rich regions, marked by arrows in Fig. 4(c), further suggesting that locally, the strain is higher there. Assuming a higher density of Ga-N bonds at the N-rich areas, from the comparison of the bond length in GaN (1.94 Å) and GaAs (2.45 Å),<sup>43</sup> it is obvious that the preferred formation of Ga-N bonds causes a higher local strain to GaAs. Note the strong resemblances between the contrast features and periodicity observed here to those on conventionally-grown Ga(As,N) [either tensile or compressively strained] attributed to nitrogen-induced strain fields.<sup>8,9</sup>

As in conventionally-grown dilute nitrides, it could be argued that the shape transition is driven by the high epitaxial tensile strain due to the increased nitrogen. The misfit epitaxial strain  $f$  arises from the difference in lattice constant between the epilayer  $a_{\text{layer}}$  and the substrate  $a_{\text{GaAs}}$ ,  $f = (a_{\text{layer}} - a_{\text{GaAs}})/a_{\text{GaAs}}$ . As previously mentioned, a similar microstructure has been found already in dilute nitrides, grown either under epitaxial compressive strain<sup>32</sup> or with a smaller tensile strain.<sup>29</sup> A representative example is shown in Figure 5 showing the morphology of a nitrogen  $\delta$ -doped GaAs/(Al,Ga)As QW with a tensile misfit strain at the insertion (assuming hypothetically 1 ML of 50% [N]) of  $f \sim -10\%$ , a nitrogen  $\delta$ -doped (In,Ga)As/GaAs QW with a tensile misfit strain of  $f \sim -5\%$ <sup>29</sup> and finally (In,Ga)(As,N)/GaAs QWs grown in the conventional way with an epitaxial compressive mismatch of  $f \sim 2\%$ ,<sup>32</sup> respectively. In all cases, regardless of the macroscopic epitaxial strain (value and sign, i.e. tensile vs. compressive), we observe a 2D-3D transition. The tensile misfit strain in the 0.12

ML  $\delta$ -doping sample (assuming 1 ML of 12% [N]), showing a 2D morphology, is about  $f \sim 2.4\%$ . Although based on the present experiments we can only speculate on the origin of the morphological transition to 3D islands, our results indicate that (i) it occurs regardless of the way nitrogen is introduced in the layers, (ii) is not driven by the macroscopic epitaxial strain since layers under tensile and compressive strain behaves similarly, and (iii) N-rich areas along the insertion are rougher, suggesting a high local strain there. Thus, in analogy to dilute nitride layers grown by conventional MBE with continuous nitrogen supply (i.e. random alloy), the 2D-3D transition in nitrogen  $\delta$ -doped layers is probably triggered by *local* strain fields originating from specific atomic configurations and, hence, it consolidates the claim that it is an intrinsic property of the material and is determined by the largely different Ga-N and Ga-As bonds.<sup>6-9</sup>

The impact of the microstructure on the optical properties of the nitrogen  $\delta$ -doped samples is also similar to that in dilute nitrides grown with continuous nitrogen supply, where there is a degradation of the photoluminescence (PL) with increasing morphological instabilities and composition fluctuations.<sup>6,9</sup> The detailed optical properties of the nitrogen  $\delta$ -doped samples are published elsewhere.<sup>14,44</sup> All samples exhibit room temperature PL although the PL intensity severely degrades with increasing roughening and composition fluctuations as the sample undergoes the 2D-3D transition. In particular, the sample with the 0.5 ML insertion shows the lowest PL intensity of the series.<sup>44</sup> The same result is found for (In,Ga)As:N<sup>14,29</sup> and, in particular, for (In,Ga)(As,N) grown in the conventional way,<sup>6,9</sup> where it is demonstrated that the highest PL efficiency is obtained for perfectly 2D-grown QWs with slightest possible composition variations.<sup>6</sup>

In summary, nitrogen sub-monolayer insertions in GaAs extend over several monolayers along the growth direction giving rise to a well-defined thin Ga(As,N) layer with in-plane and out-of-plane compositional inhomogeneities. The pronounced morphological and

chemical instabilities observed for increased nitrogen at the insertion seem to be similar to those reported in conventional dilute nitrides and be determined by material-related intrinsic factors.

This work was partly supported by a Grant-in-Aid for Young Scientists (A) from the Japan Society for the Promotion of Science and by The Research Foundation for Opto-Science and Technology. We acknowledge D. Steffen and A. Pfeiffer for technical assistance with TEM and Guanhui Gao for a careful reading of the manuscript.

ACCEPTED MANUSCRIPT

- <sup>1</sup> M. Weyers, M. Sato and H. Ando, Jpn. J. Appl. Phys. **31**, L853 (1992).
- <sup>2</sup> M. Kondow, K. Uomi, K. Hosomi and T. Mozume, Jpn. J. Appl. Phys. **33**, L1056 (1994).
- <sup>3</sup> W. Shan, W. Walukiewicz, J. W. Ager III, E. E. Haller, J. F. Geisz, D. J. Friedman, J. M. Olson and S. R. Kurtz, Phys. Rev. Lett. **82**, 1221 (1999).
- <sup>4</sup> R. S. Goldman, R.M. Feenstra, B.G. Briner, M.L. O'Steen and R.J. Hauenstein, Appl. Phys. Lett. **69**, 3698 (1995).
- <sup>5</sup> I. Suemune, N. Morooka, K. Uesugi, Y.-W. Ok and T.-Y. Seong, J. Cryst. Growth **221**, 546 (2000).
- <sup>6</sup> A. Trampert, J.-M. Chauveau, K. H. Ploog, E. Tournié and A. Guzmán, J. Vac. Sci. Technol. B **22**, 2195 (2004).
- <sup>7</sup> X. Kong, A. Trampert, E. Tournié and K. H. Ploog, Appl. Phys. Lett. **87**, 171901 (2005).
- <sup>8</sup> K. Volz, T. Torunski and W. Stolz, J. Appl. Phys. **97**, 014306 (2005).
- <sup>9</sup> I. Németh, T. Torunski, B. Kunert, W. Stolz and K. Volz, J. Appl. Phys. **101**, 123524 (2007).
- <sup>10</sup> E. Luna, F. Ishikawa, B. Satpai, J.B. Rodriguez, E. Tournié and A. Trampert, J. Cryst. Growth **311**, 1739 (2009).
- <sup>11</sup> T. Makimoto and N. Kobayashi, Appl. Phys. Lett. **67**, 688 (1995).
- <sup>12</sup> T. Kita and O. Wada, Phys. Rev. B **74**, 035213 (2006).
- <sup>13</sup> H. Zhao, S. M. Wang, Q.X. Zhao, M. Sadeghi and A. Larsson, J. Cryst. Growth **311**, 1723 (2009).
- <sup>14</sup> F. Ishikawa, M. Morifuji, K. Nagahara, M. Uchiyama, K. Higashi and M. Kondow, J. Cryst. Growth **323**, 30 (2011).
- <sup>15</sup> T. Mano, M. Jo, K. Mitsuishi, M. Elborg, Y. Sugimoto, T. Noda, Y. Sakuma and K. Sakoda, Appl. Phys. Express **4**, 125001 (2011).
- <sup>16</sup> N. Urakami, K. Yamane, H. Sekiguchi, H. Okada and A. Wakahara, J. Cryst. Growth **435**, 19 (2016).

- <sup>17</sup> K. Sumiya, M. Morifuji, Y. Oshima and F. Ishikawa, Appl. Phys. Express **6**, 041002 (2013).
- <sup>18</sup> S. Yagi, S. Noguchi, Y. Hijikata, S. Kuboya, K. Onabe and H. Yaguchi, Jpn. J. Appl. Phys. **52**, 102302 (2013).
- <sup>19</sup> T. Suzuki, K. Osada, S. Yagi, S. Naitoh, Y. Shoji, H. Hijikata, Y. Okada and H. Yaguchi, Jpn. J. Appl. Phys. **54**, 08KA07 (2015).
- <sup>20</sup> T. Kita, Y. Harada and O. Wada, Phys. Rev. B **77**, 193102 (2008).
- <sup>21</sup> M. Jo, T. Mano, T. Kuroda, Y. Sakuma and K. Sakoda, Appl. Phys. Lett. **102**, 062107 (2013).
- <sup>22</sup> M. Ikezawa, Y. Sakuma, L. Zhang, Y. Sone, T. Mori, T. Hamano, M. Watanabe, K. Sakoda and Y. Masumoto, Appl. Phys. Lett. **100**, 042106 (2012).
- <sup>23</sup> Y. Harada, T. Kubo, T. Inoue, O. Kojima and T. Kita, J. Appl. Phys. **110**, 083522 (2011).
- <sup>24</sup> M. Jo, T. Mano, Y. Sakuma and K. Sakoda, J. Appl. Phys. **115**, 123501 (2014).
- <sup>25</sup> Y. Ogawa, Y. Harada, T. Baba, T. Kaizu and T. Kita, Appl. Phys. Lett. **108**, 111905 (2016).
- <sup>26</sup> N. Nishimoto, M. Kondow and F. Ishikawa, J. Vac. Sci. Technol. B **32**(2), 02C121 (2014).
- <sup>27</sup> *Delta-Doping of Semiconductors*, edited by E. F. Schubert, (Cambridge University Press, Cambridge, 1996).
- <sup>28</sup> T. Kaizu, K. Taguchi and T. Kita, J. Appl. Phys. **119**, 194306 (2016).
- <sup>29</sup> R. Gargallo-Caballero, E. Luna, F. Ishikawa and A. Trampert, Appl. Phys. Lett. **100**, 171906 (2012).
- <sup>30</sup> N. Ishida, M. Jo, T. Mano, Y. Sakuma, T. Noda and D. Fujita, Nanoscale **7**, 16773 (2015).
- <sup>31</sup> F. Ishikawa, E. Luna, A. Trampert and K. H. Ploog, Appl. Phys. Lett. **89**, 181910 (2006).
- <sup>32</sup> A. Guzmán, E. Luna, F. Ishikawa and A. Trampert, J. Cryst. Growth **311**, 1728 (2009).
- <sup>33</sup> E. Luna, M. Wu, M. Hanke, J. Puustinen, M. Guina and A. Trampert, Nanotechnology **27**, 325603 (2016).

- <sup>34</sup> J. Lu, E. Luna, T. Aoki, E.H. Steenbergen, Y.-H. Zhang and D. J. Smith, J. Appl. Phys. **119**, 095702 (2016).
- <sup>35</sup> T. Sugitani, T. Akiyama, K. Nakamura and T. Ito, J. Cryst. Growth **378**, 29 (2013).
- <sup>36</sup> E. G. Bithell and W. M. Stobbs, Philos. Mag. A, **60**, 39 (1989).
- <sup>37</sup> J. Cagnon, P.A. Buffat, P.A. Stadelmann and K. Liefer, Inst. Phys. Conf. Ser. No. **180**, 203 (2003).
- <sup>38</sup> K. Volz, O. Rubel, T. Torunski, S.D. Baranovskii and W. Stolz, Appl. Phys. Lett. **88**, 081910 (2006).
- <sup>39</sup> Y. Harada, M. Yamamoto, T. Baba and T. Kita, Appl. Phys. Lett. **104**, 041907 (2014).
- <sup>40</sup> E. Luna, A. Guzmán, A. Trampert and G. Álvarez, Phys. Rev. Lett. **109**, 126101 (2012).
- <sup>41</sup> G.K. Vijaya, A. Freundlich, D. Tang and D. J. Smith, J. Vac. Sci. Technol. B **33(3)**, 031209 (2015).
- <sup>42</sup> A. Maros, N. Faleev, R.R. King and C.B. Honsberg, J. Vac. Sci. Technol. B **34(2)**, 02L106 (2016).
- <sup>43</sup> W. A. Harrison, *Electronic Structure and the Properties of Solids* (Dover, New York, 1989), pp. 175–176.
- <sup>44</sup> S. Furuse, K. Sumiya, M. Morifuji and F. Ishikawa, J. Vac. Sci. Technol. B **30(2)**, 02B117 (2012).

**Figure captions**

**Fig. 1.** Chemically sensitive  $g_{002}$  DFTEM micrographs of (a) a GaAs QW with a 0.12 ML N  $\delta$ -doping insertion and (b) a reference sample without the N insertion. The white arrow indicates the position of the N insertion.

**Fig. 2.** Plot of (a) the QW thickness,  $W$ ; (b) the N  $\delta$ -doping profile width,  $W_N$ ; and (c) the N content measured at different positions along the GaAs QW with a 0.12 ML N  $\delta$ -doping insertion. Note that the QW thickness fluctuations correlate with fluctuations in the width of the N  $\delta$ -doped layer  $W_N$ . On the other hand, there is an anticorrelation between the N content and the width of the N  $\delta$ -doped layer:  $W_N$  is small in areas of high  $[N]$  and vice versa, areas with low  $[N]$  extend over a larger  $W_N$ .

**Fig. 3.** (a) Chemically sensitive  $g_{002}$  DFTEM micrograph of the GaAs QW with a 0.12 ML N  $\delta$ -doping insertion, together with (b) an intensity line-scan from the area marked in (a), and (c) the nitrogen distribution profile obtained from the analysis of (b).

**Fig. 4.** Chemically sensitive  $g_{002}$  DFTEM micrographs of a GaAs QW with a 0.5 ML N  $\delta$ -doping insertion when observed along the two perpendicular (a)  $\langle 110 \rangle$  and (b)

$\langle 1\bar{1}0 \rangle$  directions. Notice the anisotropy in the layers morphology and the highly-faceted features. (c) A higher magnification  $g_{002}$  DFTEM micrograph in the  $\langle 110 \rangle$  projection with intensity line-scans along GaAs and the N  $\delta$ -doping insertion, respectively. The small black arrows indicate the presence of N-rich regions.

**Fig. 5.** Chemically sensitive  $g_{002}$  DFTEM micrographs of (a) a tensile strained N  $\delta$ -doped GaAs/(Al,Ga)As QW structure, (b) a tensile strained N  $\delta$ -doped (In,Ga)As/GaAs QW structure and (c) compressively strained (In,Ga)(N,As)/GaAs QWs grown with continuous

nitrogen supply. The samples exhibit a similar microstructure with highly-faceted 3D structures.

ACCEPTED MANUSCRIPT

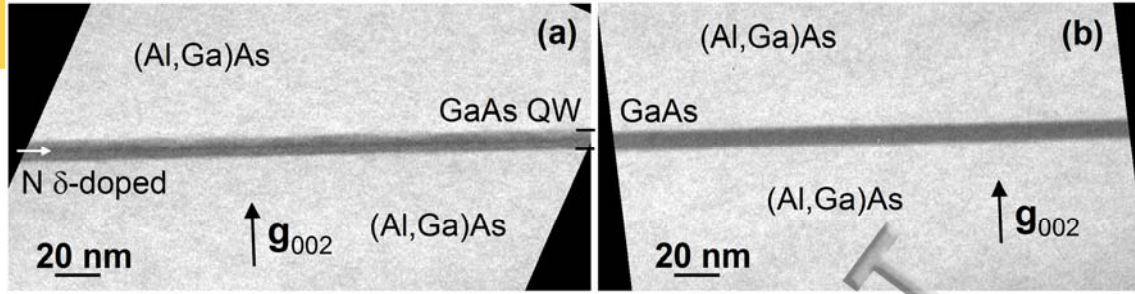


**Figure 1.** (Color online) E. Luna *et al.*

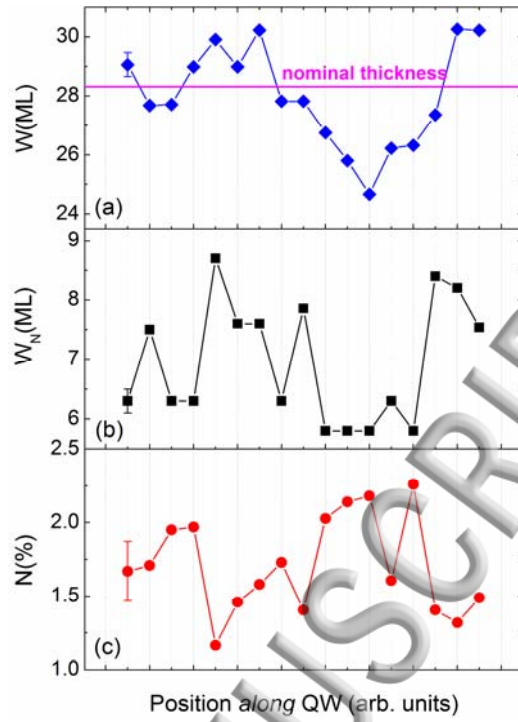


Figure 2. (Color online) E. Luna *et al.*.

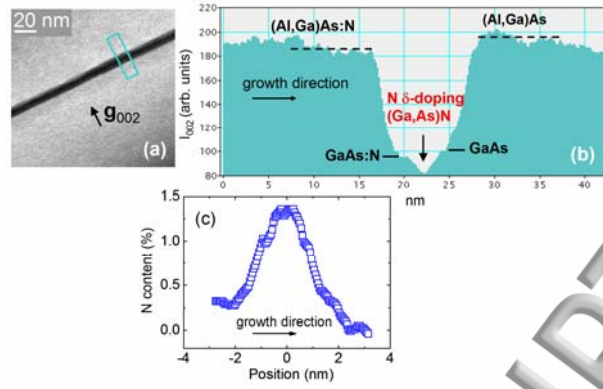


Figure 3. (Color online) E. Luna *et al.*

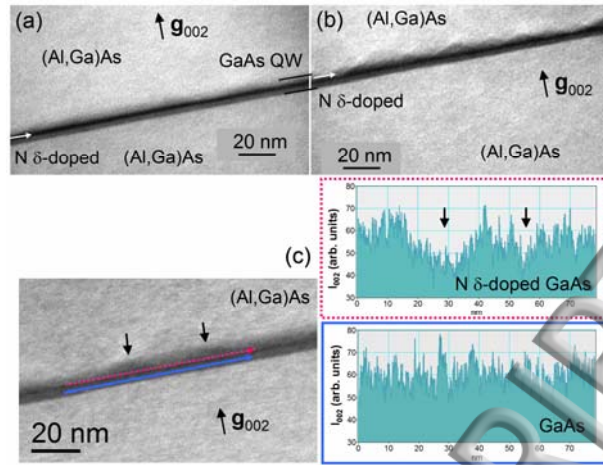
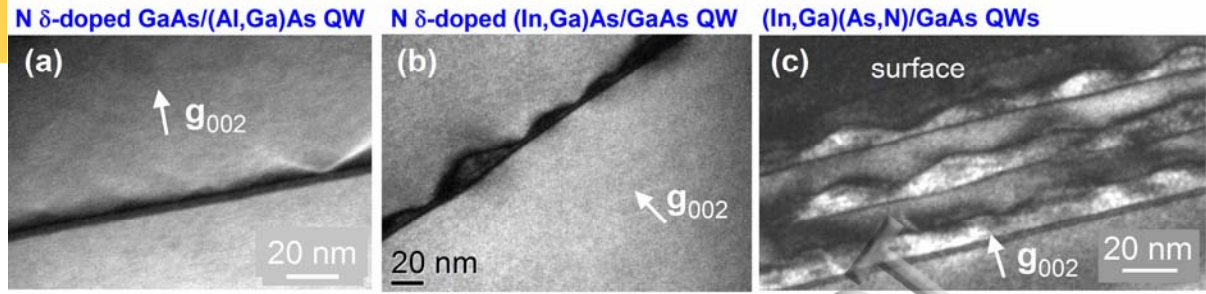
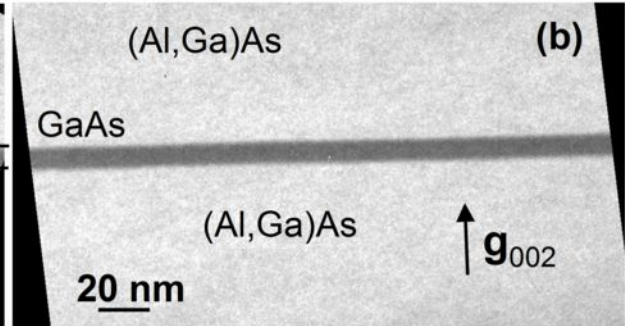
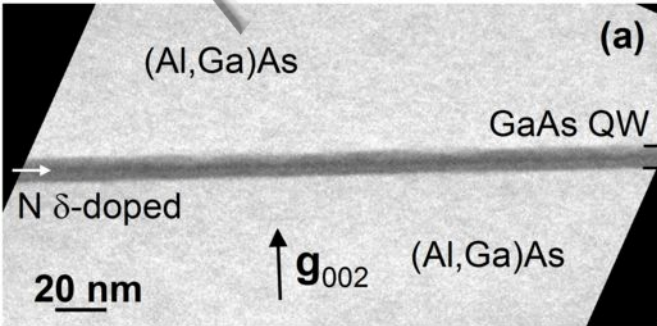


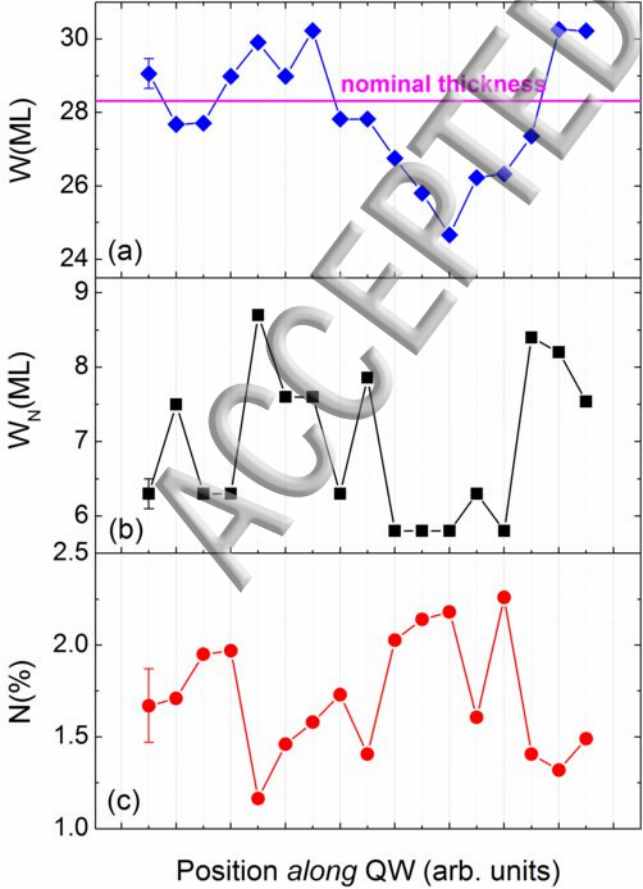
Figure 4. (Color online) E. Luna *et al.*.

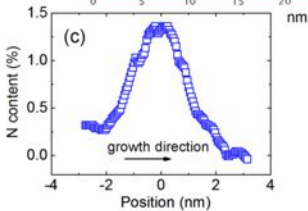
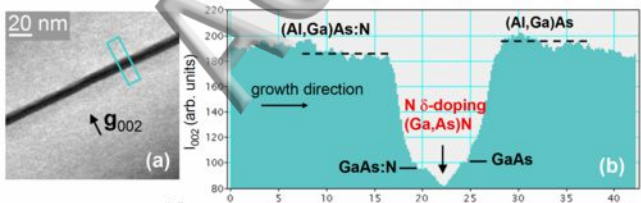


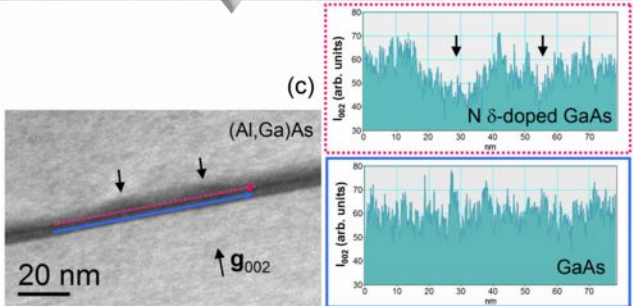
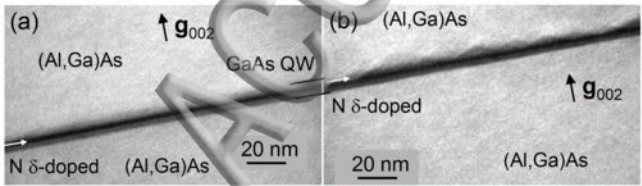
**Figure 5.** (Color online) E. Luna *et al.*

ACCEPTED MANUSCRIPT

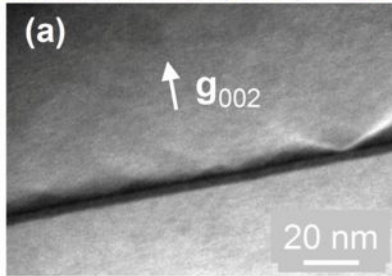




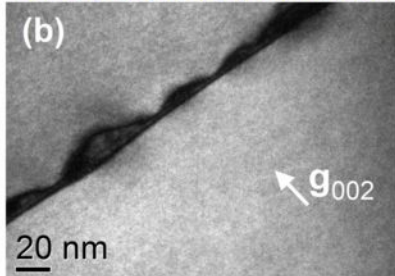




**N  $\delta$ -doped GaAs/(Al,Ga)As QW**



**N  $\delta$ -doped (In,Ga)As/GaAs QW**



**(In,Ga)(As,N)/GaAs QWs**

